Published in final edited form as:
J Am Chem Soc. 2008 October 15; 130(41): 13709–13717. doi:10.1021/ja804087r.

Anionic Snieckus-Fries Rearrangement:

Solvent Effects and Role of Mixed Aggregates

Jason C. Riggs, **Kanwal J. Singh**, **Ma Yun**, and **David B. Collum**
Contribution from the Department of Chemistry and Chemical Biology Baker Laboratory, Cornell University, Ithaca, New York 14853-1301

Abstract

Lithiated aryl carbamates (ArLi) bearing methoxy or fluoro substituents in the meta position are generated from lithium diisopropylamide (LDA) in THF, *n*-BuOMe, Me_2NEt, dimethoxyethane (DME), *N*,*N*,*N'*,*N'*-tetramethylethylenediamine (TMEDA), *N*,*N*,*N'*,*N'*-tetramethylcyclohexanediamine (TMCDA), and hexamethylphosphoramide (HMPA). The aryllithiums are shown with ^{6}Li, ^{13}C, and ^{15}N NMR spectroscopies to be monomers, ArLi-LDA mixed dimers, and ArLi-LDA mixed trimers, depending on the choice of solvent. Subsequent Snieckus-Fries rearrangements afford ArOLi-LDA mixed dimers and trimers of the resulting phenolates. Rate studies of the rearrangement implicate mechanisms based on monomers, mixed dimers, and mixed trimers.

Introduction

The anionic Snieckus-Fries rearrangement of aryl carbamates (eq 1) is a highly effective means of carrying out orthosubstitutions.[1,2] Its popularity stems in large part from the dogged determination of Snieckus and coworkers to optimize the protocol and expand the scope of the reaction (which prompts us to cast a vote for adding Snieckus to the name).[3-6]

E-Mail: dbc6@cornell.edu.

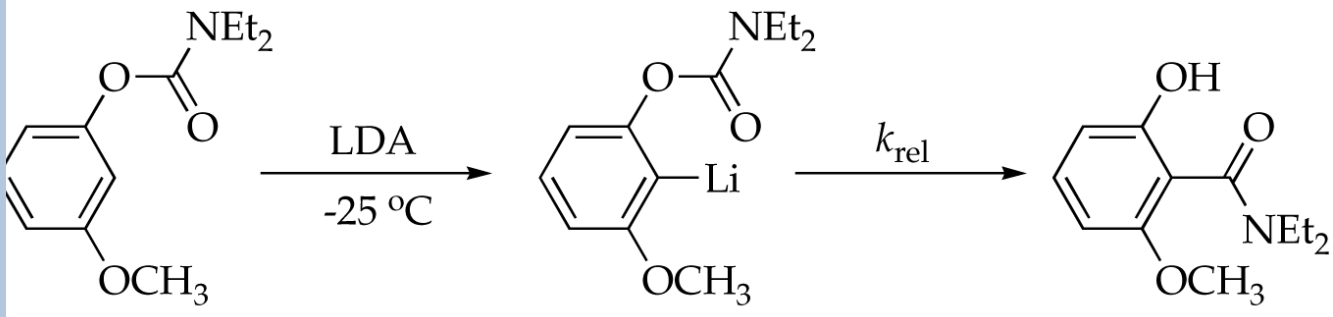

solvent[3]	yield	k_{rel}
THF	88%	5
THF/HMPA	84%	7700
n-BuOMe	83%	1
DME	94%	90
TMCDA	87%	90
TMEDA	83%	12
Me_2NEt	88%	2

(1)

Our interest in the Snieckus-Fries rearrangement was piqued by its probative value to study organolithium structure-reactivity relationships. Dimethylcarbamates bearing no meta substituent favor rapid intramolecular acyl transfer, affording insight into only the slow (rate limiting) ortholithiation step.[7] By contrast, aryl carbamates bearing activating meta substituents (OCH_3 or F) and bulky carbamoyl groups rapidly form a relatively stable intermediate aryllithium, allowing the rearrangement step to be examined as well.[8]

The consistently high yields accompanying eq 1 suggest that the choice of coordinating solvent is unimportant, but yields offer little insight into reactivity.[9] The relative rate constants (k_{rel}) show that the choice of coordinating solvent markedly influences the rate of acyl transfer. Of course, solvent-dependent relative reactivities do not offer direct insights into underlying organolithium structures and reaction mechanisms.[10,11]

In a previous study we investigated reactivities and mechanisms of the ortholithiation of aryl carbamates, paying only limited attention to the acyl transfer.[7] This paper focuses exclusively on the acyl transfer. We describe herein studies of solvent-dependent structures of the intermediate lithiated aryl carbamates and evidence of monomer-, mixed dimer-, and mixed

trimer-based mechanisms for the rearrangement.[12] The mixed *trimer*-based pathway may represent the first documented example of an organolithium reaction in which the rate-limiting transition structure is *more* highly aggregated than the reactants.[13]

Results

A series of structural, kinetic, and computational studies are described below. The choice of substrates was not as arbitrary as it might seem. Rate studies demand structural homogeneity to maximize the clarity of the results.[11,14] The wide range of solvent-dependent reactivities foreshadowed by eq 1 demanded tinkering with the carbamoyl group and meta substituent to optimize the protocol for characterizing the starting aryllithiums and monitoring the rearrangements. General descriptions of protocols are followed by specific results organized according to solvent.

Structural Studies

Lithium diisopropylamide (LDA), [^{6}Li]LDA, and [^{6}Li,^{15}N]LDA were prepared as white crystalline solids.[15,16] Previous investigations of LDA solvated by THF, *n*-BuOMe, THF/HMPA, and Me_2NEt have revealed dimers **1a-d** as the sole observable forms.[3,17a,d] Bifunctional ligands DME and TMEDA afford non-chelated dimers **2a** and **2b**, respectively.[3,17b,c] LDA solvated by TMCDA forms exclusively monomer **3**.[3,17b]

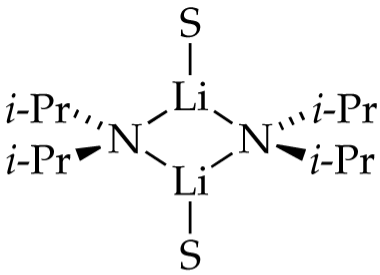

1a; S = THF
1b; S = *n*-BuOMe
1c; S = HMPA
1d; S = Me_2NEt

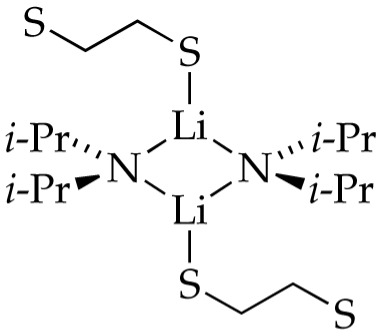

2a; S = OMe (DME)
2b; S = NMe_2 (TMEDA)

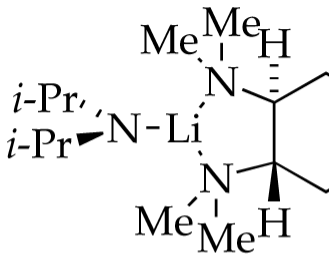

3

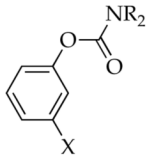

4a; R= Me, X = OMe
4b; R = Et, X = OMe
4c; R = *i*-Pr, X = OMe
4d; R = Me, X = F
4e; R= *i*-Pr, X= F

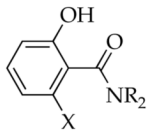

5a; R = Me, X = OMe
5b; R = Et, X = OMe
5c; R = Me, X = F

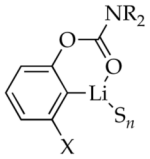

6a; S = THF, R = *i*-Pr, X = F
6b; S = HMPA, R = Et, X = OMe
6c; S = HMPA, R = *i*-Pr, X = OMe
6d; S = HMPA, R = Me, X = F
6e; S = HMPA, R = *i*-Pr, X = F
6f; S = DME, R = *i*-Pr, X = F
6g; S = η^2-TMCDA, R = Et, X = OMe

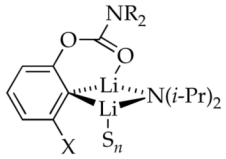

7a; S = THF, R = Me, X = F
7b; S = THF, R = *i*-Pr, X = F
7c; S = *n*-BuOMe, R = Me, X = F
7d; S = *n*-BuOMe, R = Et, X = OMe
7e; S = DME, R = Me, X = F
7f; S = DME, R= *i*-Pr, X= F
7g; S = η^1-TMEDA, R = *i*-Pr, X = OMe
7h; S = Me_2NEt, R = Et, X = OMe

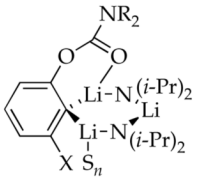

8a; S = η^1-TMEDA, R = *i*-Pr, X = OMe
8b; S = Me_2NEt, R = Et, X = OMe

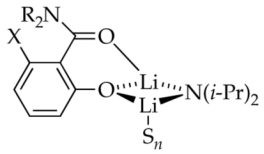

9a; S = THF, R = Me, X = F
9b; S = *n*-BuOMe, R = Et, X = OMe
9c; S = HMPA, R = Et, X = OMe
9d; S = HMPA, R = Me, X = F

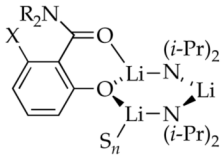

10a; S = *n*-BuOMe, R = Et, X = OMe
10b; S = HMPA, R = Et, X = OMe
10c; S = DME, R = Me, X = F
10d; S = η^1-TMEDA, R = Me, X = OMe
10e; S = Me_2NEt, R = Et, X = OMe

Aryllithiums **6a-g**, mixed dimers **7a-h**, and mixed trimers **8a-b** were generated from aryl carbamates **4a-e**[18] using [^{6}Li]LDA or [^{6}Li,^{15}N]LDA. Rearrangement in the presence of excess LDA affords phenolate-based mixed dimers **9a-d** and mixed trimers **10a-e**, which were synthesized independently by lithiating phenols **5a-c** with excess [^{6}Li,^{15}N]LDA.

The structural assignments stem from splitting patterns observed using one-dimensional ^{6}Li, ^{15}N, and ^{13}C NMR spectroscopies[17a] as well as ^1J(^{6}Li,^{15}N)-resolved[19] and ^{6}Li,^{15}N-HSQC NMR spectroscopies.[20] Spectroscopic data are summarized in Table 1, and spectra are archived in supporting information. Although the structures and affiliated equilibria are complex, the methods used are well established. In lieu of detailed descriptions

of the assignments for each solvent-substrate-aggregate combination, a few general statements should suffice.

1. Some monomeric aryllithiums could be generated only by using 1.0 equiv of [^{6}Li,^{15}N]LDA in some cases (**6a** and **6f**) whereas other monomers are formed even with excess [^{6}Li,^{15}N]LDA (**6b-e** and **6g**). The anticipated ^{6}Li-^{13}C coupling is seen by ^{13}C NMR spectroscopy in some cases, but most show only broad mounds. We have noted, however, that mixtures of such putative aryllithium monomers do not form ArLi-Ar'Li heteroaggregates,[21] consistent with the monomer assignment.[22] Previous spectroscopic studies strongly support a prevalence of monomers.[23-25] Especially large $^{2}J_{FC}$ couplings (>100 Hz) in the ^{13}C NMR spectra are similar to those observed in other orthofluorinated aryllithiums.[7,23a,23b,26]

2. Mixed dimers (**7**) available by using excess [^{6}Li,^{15}N]LDA show characteristic ^{6}Li doublets and ^{15}N quintets consistent with the Li_a-N_b-Li_c connectivity. The asymmetry imparted by chelation of the carbamate moiety could be observed as two ^{6}Li resonances at very low temperature (<-125 °C). ^{13}C NMR spectra show quintets due to coupling of the lithiated carbon to two ^{6}Li nuclei and, in the case of the meta fluoro species, are further split by J_{FC} coupling.

3. Mixed trimers (**8**) display three ^{6}Li resonances in a 1:1:1 ratio, manifesting the ^{6}Li-^{15}N coupling consistent with a Li_a-N_b-Li_c-N_d-Li_e subunit. Each mixed trimer also displays a triplet of triplets and a quintet in the ^{15}N NMR spectrum. The asymmetry confirms the chelation of the carbamate moiety as drawn.

4. Phenolate mixed dimers (**9**) display characteristic ^{6}Li doublets and ^{15}N quintets that are consistent with Li_a-N_b-Li_c connectivity. The ^{6}Li resonances of the phenolate mixed dimers are upfield from the aryllithium mixed dimers (**7**).

5. Phenolate mixed trimers (**10**) show three ^{6}Li resonances as two doublets and one triplet in a 1:1:1 ratio. Two ^{15}N resonances appear as either triplet of triplets or quintets.[7,27]

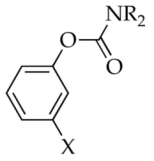

4a; R= Me, X = OMe
4b; R = Et, X = OMe
4c; R = *i*-Pr, X = OMe
4d; R = Me, X = F
4e; R= *i*-Pr, X= F

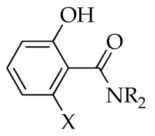

5a; R = Me, X = OMe
5b; R = Et, X = OMe
5c; R = Me, X = F

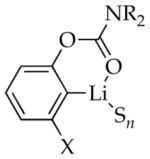

6a; S = THF, R = *i*-Pr, X = F
6b; S = HMPA, R = Et, X = OMe
6c; S = HMPA, R = *i*-Pr, X = OMe
6d; S = HMPA, R = Me, X = F
6e; S = HMPA, R = *i*-Pr, X = F
6f; S = DME, R = *i*-Pr, X = F
6g; S = η^2-TMCDA, R = Et, X = OMe

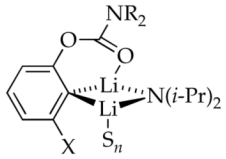

7a; S = THF, R = Me, X = F
7b; S = THF, R = *i*-Pr, X = F
7c; S = *n*-BuOMe, R = Me, X = F
7d; S = *n*-BuOMe, R = Et, X = OMe
7e; S = DME, R = Me, X = F
7f; S = DME, R= *i*-Pr, X= F
7g; S = η^1-TMEDA, R = *i*-Pr, X = OMe
7h; S = Me_2NEt, R = Et, X = OMe

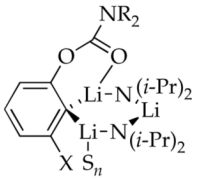

8a; S = η^1-TMEDA, R = *i*-Pr, X = OMe
8b; S = Me_2NEt, R = Et, X = OMe

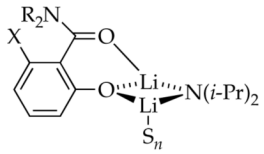

9a; S = THF, R = Me, X = F
9b; S = *n*-BuOMe, R = Et, X = OMe
9c; S = HMPA, R = Et, X = OMe
9d; S = HMPA, R = Me, X = F

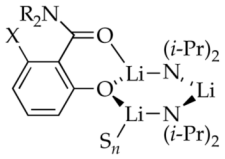

10a; S = *n*-BuOMe, R = Et, X = OMe
10b; S = HMPA, R = Et, X = OMe
10c; S = DME, R = Me, X = F
10d; S = η^1-TMEDA, R = Me, X = OMe
10e; S = Me_2NEt, R = Et, X = OMe

Rate Studies: General Methods[11,28,29]

The anionic Snieckus-Fries rearrangement was monitored using an in situ IR spectrometer fitted with a 30-bounce, silicon-tipped probe.[30] The carbonyl group provided an excellent handle for following the loss of the aryllithium (monomer **6** or mixed dimer **7**; 1670-1690 cm^{-1}) and the growth of the aryl carboxamide (**9** or **10**; 1590-1610 cm^{-1}). Pseudo-first-order conditions were established by maintaining the aryllithium concentration at 0.004 M. Mixed dimers **7a**, **7d**, and **7e** and monomers **6b**, **6d**, and **6g** were generated in situ with excess LDA. Solvent concentrations were high, yet adjustable, using a cosolvent (pentane, hexane, or toluene).[31] The resulting pseudo-first-order rate constants (k_{obsd}) are independent of the initial

concentration of the aryllithium, confirming a first-order dependence. The decays also follow first-order dependencies, as shown by least-squares fits to the nonlinear Noyes equation.[32] Phenolate-based mixed aggregates **9** and **10** or any unforeseen conversion-dependent changes were shown to be inconsequential under the pseudo-first-order conditions by reestablishing the baseline at the end of a run, injecting a second aliquot of aryl carbamate, and confirming that the first and second rate constants are equivalent (±10%). The reaction orders are summarized in Table 2.

Computations

Calculations based on density functional theory (DFT) were performed at the B3LYP/6-31G (d) level of theory using Gaussian 03 and visualized with GaussView 3.09.[33] Gibbs free energies (ΔG^{o}, kcal/mol) include thermal corrections at 298 K. Calculated transition structures were shown to be legitimate saddle points by the existence of a single imaginary frequency. The alkyl groups on the carbamate were modeled as methyl groups, and LDA was modeled as lithium dimethylamide. THF and *n*-BuOMe were modeled as dimethylether (Me_2O). TMCDA was modeled as TMEDA. The results, comprising 43 calculated reactants and 23 calculated transition structures, are archived in supporting information. Selected observations are presented in the context of the specific solvents as described below.

THF

The metalation of **4d** and subsequent rearrangement in THF solution were studied previously;[7] the results are summarized to provide context. Rearrangement of mixed dimer **7a** in THF and excess LDA affords LDA-lithium phenolate mixed dimer **9a**. The idealized rate law[34] for the rearrangement (eq 2) is consistent with parallel pathways via transition structures **11** and **12** (eq 3). Computations using Me_2NLi/Me_2O suggest that **7a** is a monosolvated mixed dimer as drawn and they support **11** and **12** implicated by the rate law are reasonable.

$$-d[7\mathbf{a}]/dt = k'[7\mathbf{a}][\mathrm{THF}]^{1}[\mathrm{LDA}]^{0} + k''[7\mathbf{a}][\mathrm{THF}]^{2}[\mathrm{LDA}]^{-1/2} \quad (2)$$

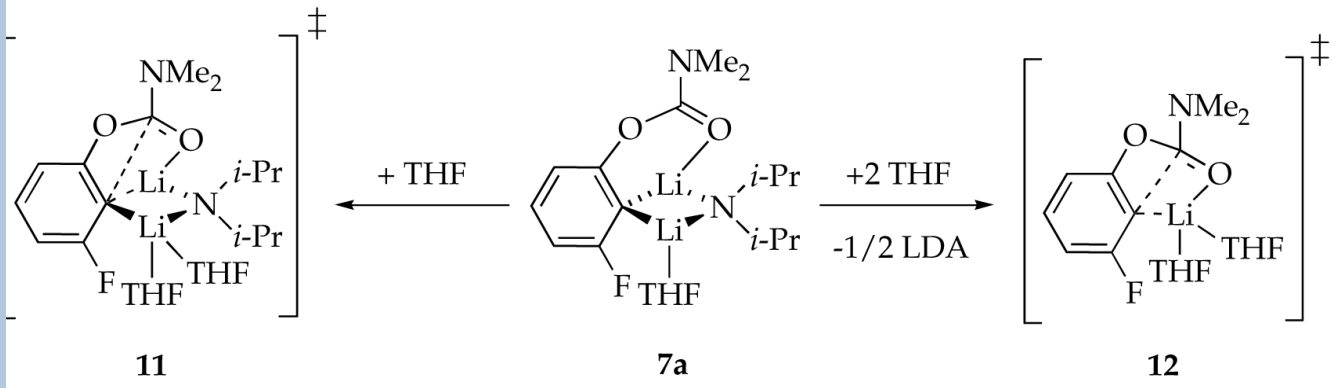

11 **7a** **12**

(3)

n-BuOMe

Lithiation of **4b** with excess LDA/*n*-BuOMe affords mixed dimer **7d** as the only observable form. Solvation numbers cannot be ascertained spectroscopically, but DFT computations (see supporting information) suggest that monosolvated mixed dimer **7d** is favored. Rearrangement of **7d** in *n*-BuOMe with excess LDA affords LDA-lithium phenolate mixed dimer **9b** and mixed trimer **10a**.

A plot of k_{obsd} versus *n*-BuOMe concentration (Figure 1) for the rearrangement of mixed dimer **7d** reveals two limiting behaviors: (1) an *inverse* dependence on *n*-BuOMe concentration,

which is consistent with a mechanism requiring solvent dissociation, and (2) a zeroth-order dependence on *n*-BuOMe concentration, indicating a nondissociative mechanism. Plots of k_{obsd} versus LDA concentration (Figures 2 and 3) show a *positive* half-order LDA dependence with a non-zero intercept at low *n*-BuOMe concentration (affiliated with the mechanism requiring solvent dissociation) and a zeroth-order LDA dependence at high *n*-BuOMe concentration (affiliated with the nondissociative mechanism). The reaction orders are consistent with the idealized rate law in eq 4, the mechanisms described generically in eq 5-7, and transition structures **13** and **14** (eq 8). Although mixed dimer **7d** is the observable form, the Snieckus-Fries rearrangement is *faster* via mixed *trimer*-based transition structure **13**. Calculations using Me_2NLi/Me_2O support both **13** and **14** as viable and suggest a greater preference for **13** (although such a non-isodesmic comparison should be made with caution if at all).

$$-d[7\mathbf{d}]/dt = k'[7\mathbf{d}][n-\mathrm{BuOMe}]^{-1}[\mathrm{LDA}]^{1/2} + k''[7\mathbf{d}][n-\mathrm{BuOMe}]^{0}[\mathrm{LDA}]^{0} \quad (4)$$

$$(i-\mathrm{Pr_2NLi})\underset{(7\mathbf{d})}{(\mathrm{ArLi})}(n-\mathrm{BuOMe}) + 1/2\,(i-\mathrm{Pr_2NLi})_2(n-\mathrm{BuOMe})_2 \leftrightarrows \bullet(i-\mathrm{Pr_2NLi})_2(\mathrm{ArLi})(n-\mathrm{BuOMe}) + n-\mathrm{BuOMe} \quad (5)$$

$$(i-\mathrm{Pr_2NLi})_2(\mathrm{ArLi})(n-\mathrm{BuOMe}) \rightarrow [(i-\mathrm{Pr_2NLi})_2(\mathrm{ArLi})(n-\mathrm{BuOMe})]^{\ddagger}_{(13)} \quad (6)$$

$$\underset{(7\mathbf{d})}{(i-\mathrm{Pr_2NLi})(\mathrm{ArLi})}(n-\mathrm{BuOMe}) \rightarrow [\underset{(14)}{(i-\mathrm{Pr_2NLi})(\mathrm{ArLi})}(n-\mathrm{BuOMe})]^{\ddagger} \quad (7)$$

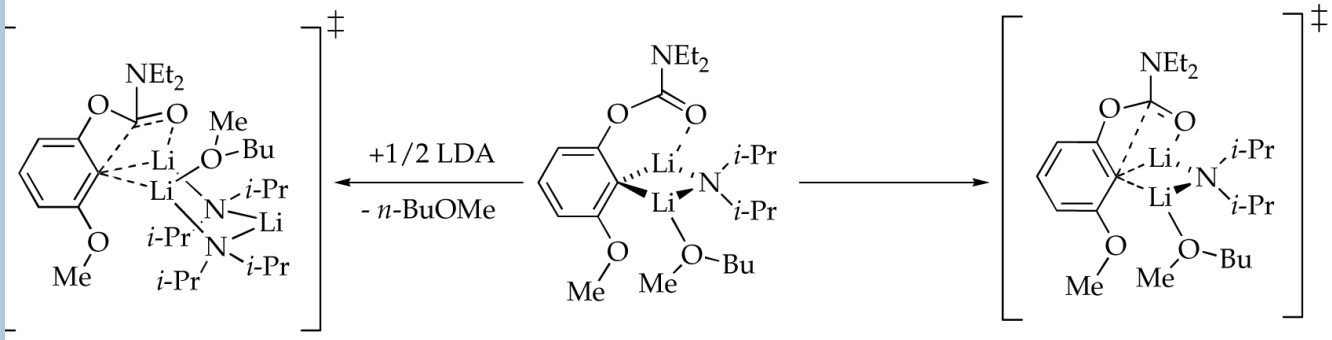

(8)

HMPA

Metalation of **4c** and **4e** with LDA/HMPA/THF affords monomers **6c** and **6e** to the exclusion of mixed aggregates even with excess LDA.[35] Unfortunately, $^1J_{CLi}$ coupling was not observed in the ^{13}C NMR spectra. ^6Li-^{31}P coupling was also absent.[36] Rearrangement of **6b** in HMPA/THF and excess LDA affords LDA-lithium phenolate mixed dimer **9c** and mixed trimer **10b**. By contrast, rearrangement of **6d** in HMPA/THF and excess LDA affords only LDA-lithium phenolate mixed dimer **9d**.

A plot of k_{obsd} versus HMPA concentration (Figure 4) for the rearrangement of monomer **6b** reveals a first-order dependence on HMPA concentration (with a relatively minor non-zero intercept) consistent with a dominant mechanism requiring solvation by one additional HMPA. Plots of k_{obsd} versus LDA concentration and k_{obsd} versus THF concentration reveal zeroth-order dependencies. The idealized rate law (eq 9) is consistent with the mechanisms described generically in eq 10 and transition structure **15**. Analogous results are obtained using the fluorinated aryllithium monomer **6d**, albeit at approximately threefold slower rearrangement

rates, presumably due to inductive stabilization. Similar relative reactivities of MeO- and F-substituted aryllithiums were observed for the elimination of lithium halides to form benzynes.[23b]

$$-d[\mathbf{6b}]/dt = k'[\mathbf{6b}][\mathrm{HMPA}]^1[\mathrm{THF}]^0[\mathrm{LDA}]^0 \quad (9)$$

$$\underset{(\mathbf{6b})}{(\mathrm{ArLi})(\mathrm{HMPA})_n} + \mathrm{HMPA} \rightarrow [(\mathrm{ArLi})(\mathrm{HMPA})_{n+1}]^{\ddagger(15)} \quad (10)$$

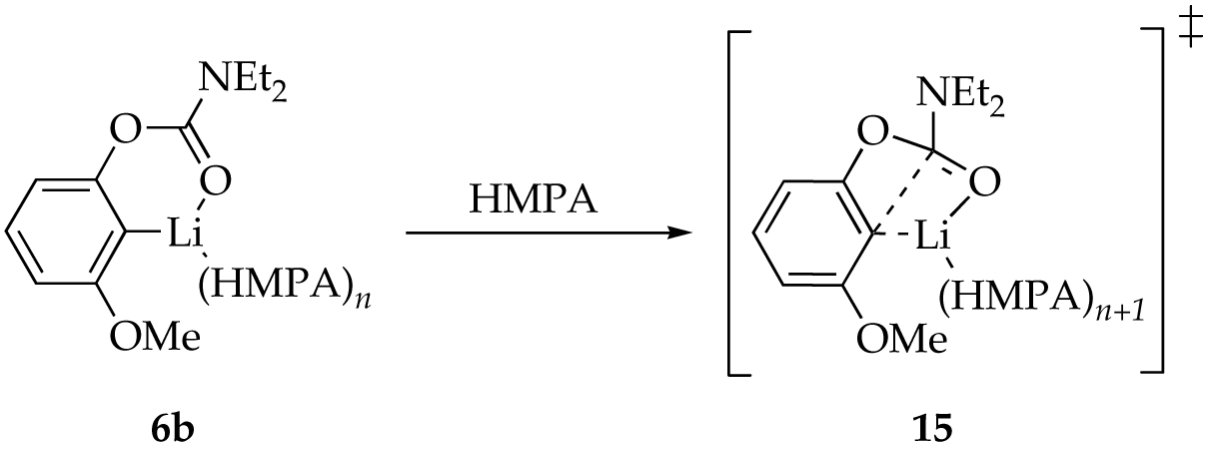

6b **15** (11)

DME

Lithiation of **4e** with excess LDA/DME affords mixed dimer **7f** as the sole observable aggregate. Unlike *n*-BuOMe, DME can be η^1- or η^2-coordinated in either the reactant or the transition structure. DFT computations indicate that (1) the substitution of *n*-BuOMe by η^1-coordinated DME is nearly thermoneutral (eq 12), and (2) the η^2-coordinated mixed dimer (**18**) is 5.1 kcal/mol favored over the η^1-coordinated mixed dimer **17** (eq 13). One Li-C bond of η^2-coordinated mixed dimer **18** is long (2.88 Å) with an accompanying shortening of the Li-F contact, however, suggesting cleavage (ring expansion) to accommodate the second oxygen of DME. Although the calculations are provocative, the veracity of **18** is undermined by experimental binding studies (discussed below). The open dimer motif of **18**, however, resurfaces in the context of the rate studies described below.

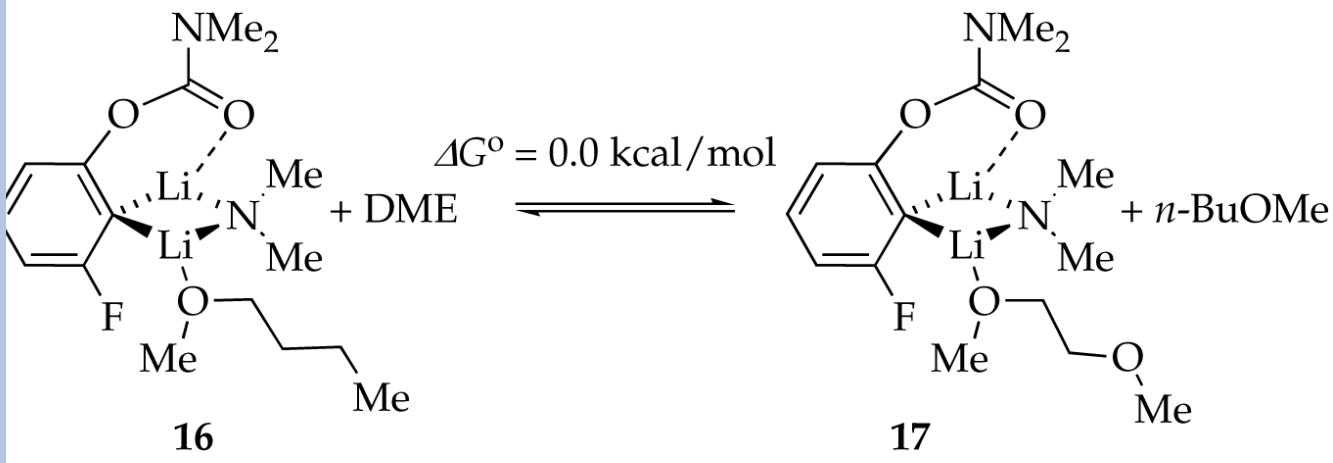

16 **17** (12)

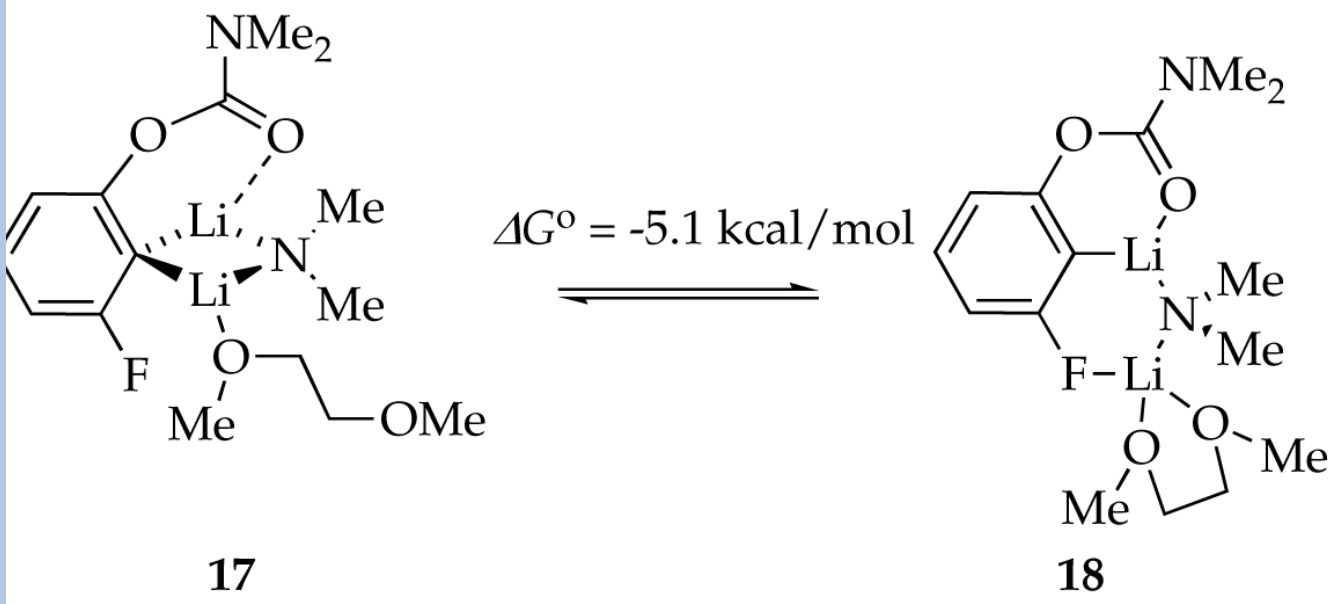

17 **18**

(13)

Plots of k_{obsd} versus DME concentration and k_{obsd} versus LDA concentration for the rearrangement of mixed dimer **7e** reveal that the rearrangement is *independent* of both the DME and LDA concentrations. The reaction orders are consistent with the idealized rate law in eq 14, the mechanism described generically in eq 15, and transition structure **19**. Notably, the reaction is much faster (approximately *90 times* in eq 1) than it is in neat *n*-BuOMe. The origins of the acceleration are instructive about the role of chelation in the reactant **7e** and transition structure **19**.

$$-d[7\mathbf{e}]/dt = k'[7\mathbf{e}][\mathrm{DME}]^0[\mathrm{LDA}]^0 \tag{14}$$

$$\underset{(7\mathbf{e})}{(i-\mathrm{Pr_2NLi})(\mathrm{ArLi})(\mathrm{DME})} \rightarrow \left[\underset{(19)}{(i-\mathrm{Pr_2NLi})(\mathrm{ArLi})(\mathrm{DME})}\right]‡ \tag{15}$$

To understand the binding of DME in mixed dimer **7e** we experimentally measured the relative binding energies of *n*-BuOMe and DME using a variation of a Job plot as follows.[37] The rearrangement was carried out in DME/*n*-BuOMe mixtures according to Scheme 1. The total concentration of DME and *n*-BuOMe is held fixed at 5.0 M. The proportion is expressed as a mole fraction of DME, X. The observed rate constant is described as a function of the mole fraction according to eq 16. Three possible limiting results are illustrated in Figure 5. If *n*-BuOMe and DME bind equivalently (K_{eq} = 1), a plot of k_{obsd} versus mole fraction of DME will be linear. If chelation causes DME to be a superior ligand (K_{eq} = 10), then the rate will rise and saturate at relatively low DME concentrations. In the unlikely event that *n*-BuOMe is superior to DME as a ligand for the mixed dimer (K_{eq} = 0.1), then the opposite curvature will be observed.

$$k_{obsd} = \left[k_{BuOMe} + \left(k_{DME}K_{eq} - k_{BuOMe}\right)X_{DME}\right] / \left[1 + \left(K_{eq} - 1\right)X_{DME}\right] \tag{16}$$

The data in Figure 6 shows curvature consistent with slight preference for solvation by DME compared to *n*-BuOMe (·G^o = -0.2 kcal/mol). Therefore, either η^2-coordinated DME is not present, or the η^1 and η^2 forms are isoenergetic. For the sake of further discussion, we depict **7e** as containing unchelated DME as drawn. Although it is unclear why the computations (cf.

17 and **18**) are so poorly predictive (the Me_2NLi model could be at fault), the potential importance of the fluoro moiety to stabilize ring-expanded (open) dimers resurfaces (vide infra).

The nearly equal binding energies of *n*-BuOMe and DME in the reactant and 90-fold acceleration of the rearrangement suggest that DME is chelated in the transition state illustrated in eq 17. Such "hemilability" of DME-solvated LDA has been documented on several occasions.[38] Computations show a significant preference for the chelated form with affiliated ring expansion, as illustrated in eq 18. (Recall that caution is warranted here.)

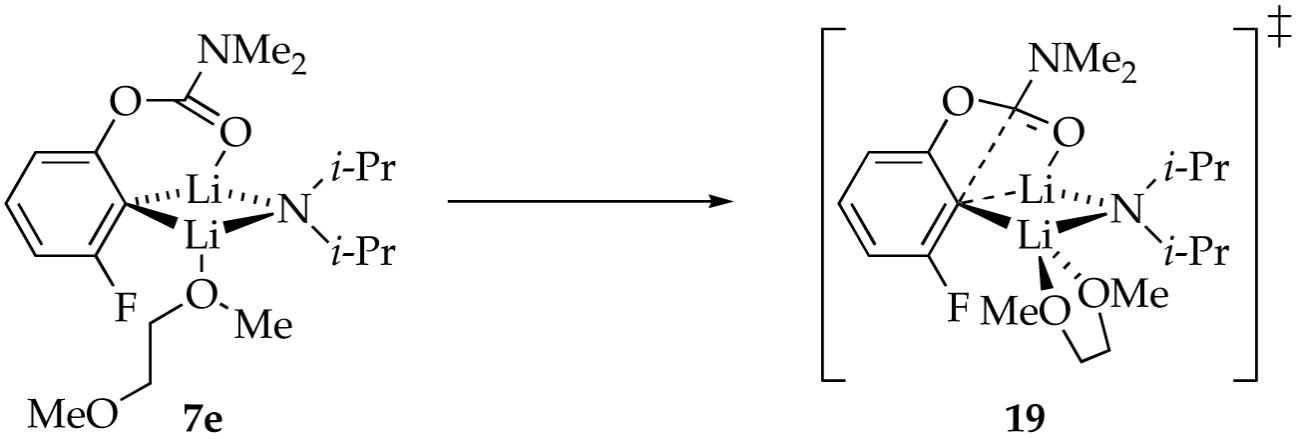

(17)

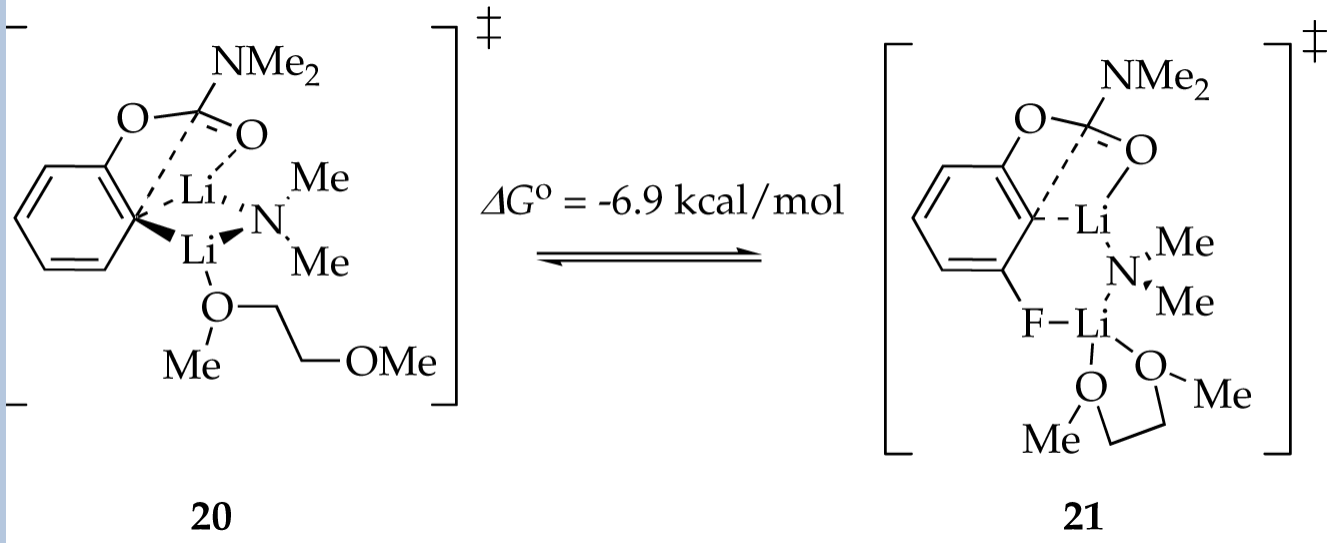

(18)

TMEDA and Me_2NEt

TMEDA surprisingly affords both mixed dimer **7g** and mixed trimer **8a**. We believed that chelation would disfavor trimers. Is TMEDA failing to chelate? Possibly. Me_2NEt, a non-chelating analog of TMEDA, also affords mixed dimer and trimer (**7h** and **8b**). Fries rearrangement of the mixed dimers and trimers in TMEDA and Me_2NEt with excess LDA yield trimers **10d** and **10e**. Rate studies using mixtures of starting materials are generally ill advised and were not pursued.

TMCDA

To study the role of a chelating diamine on the reaction rate and mechanism, we investigated TMCDA as a strongly coordinating model of TMEDA. Metalation of **4b** with LDA/TMCDA affords only monomer **6g** even with excess LDA. This substantial change in structure, when compared with the results using TMEDA, suggests that TMCDA chelates and TMEDA does not. Monomer **6g** displays a characteristic ^{6}Li singlet and ^{13}C triplet. We were not, however, able to observe free and bound TMCDA using ^{13}C NMR spectroscopy. DFT calculations using, ironically, TMEDA as a model for TMCDA suggest that the chelate is plausible. Rearrangement of **6g** at -25 °C affords a complex mixture of phenoxides. The complexity of the product distribution does not preclude detailed rate studies, however.

Plots of k_{obsd} versus TMCDA concentration and k_{obsd} versus LDA concentration for the rearrangement of monomer **6g** reveal zeroth-order dependencies. The idealized rate law in eq 19 is consistent with a single mechanism requiring no net changes in aggregation or solvation described generically in eq 20 and transition structure **22** (eq 21).[39]

$$-d[\mathbf{6g}]/dt = k'[\mathbf{6g}][\mathrm{TMCDA}]^0[\mathrm{LDA}]^0 \tag{19}$$

$$\underset{(\mathbf{6g})}{(\mathrm{ArLi})(\mathrm{TMCDA})} \rightarrow \underset{(\mathbf{22})}{[(\mathrm{ArLi})(\mathrm{TMCDA})_1]^{\ddagger}} \tag{20}$$

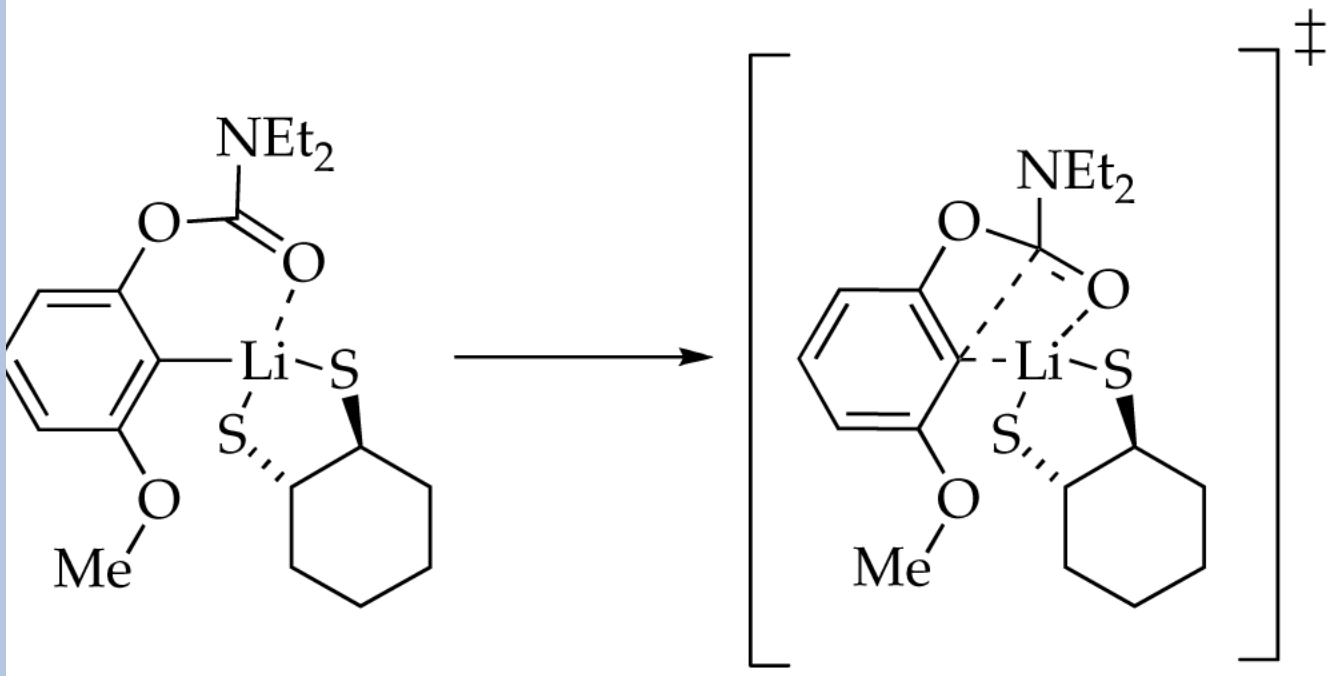

6g (S=NMe$_2$) **22** (S=NMe$_2$)

(21)

Discussion

We introduced the work described herein with solvent-dependent yields and rates of an archetypal Snieckus-Fries rearrangement shown in eq 1. Noting that yields do not shed light on rates, and simple relative rate constants do not shed light on causative organolithium

structures and mechanisms, we embarked on studies of solvent-dependent structure-reactivity relationships. Control over both reactant structures and reaction rates--two important requisites of transparent mechanistic studies--demanded taking liberties in the choice of carbamoyl group and meta substituent. A coherent summary of the results, however, requires that we also take some linguistic liberties by largely ignoring the substrate variations and focusing on the influence of solvent. Scheme 2 summarizes these results. We do not wish to imply, however, that fluoro and methoxy moieties are interchangeable; substrate-dependent changes in mechanism may lurk undetected under the surface. The structures of the reactants assigned spectroscopically and the putative transition structures are supported by computations that are largely archived in supporting information.

Solution Structures

The solvent dependent structures of lithiated aryl carbamates follow fairly conventional patterns. The most strongly coordinating solvents such as TMCDA and HMPA promote monomers (**6**). The most strongly coordinating ethereal solvent (THF) can afford monomers, but affords mixed dimers (**7**) with excess LDA. The less strongly coordinating *n*-BuOMe promotes exclusively mixed dimers, whereas the very weakly coordinating Me_2NEt[10a, 10c, 17c,40] affords mixtures of mixed dimers and mixed trimers. (Mixed trimers are generally favored by weakly coordinating solvents because of their relatively low perlithium solvation numbers.)[7,17a,41,42] Previous studies, however, have shown that TMEDA is superior to DME as a chelating ligand.[43] By the simple paradigm that solvation energy correlates with aggregation state, therefore, DME appears to be a stronger ligand than TMEDA given that TMEDA affords mixed dimers and trimers. Indeed, tacit evidence suggests that TMEDA is too sterically demanding to chelate mixed dimer **7**, causing TMEDA to function equivalently to the poorly coordinating Me_2NEt.[44] On many occasions we have found that the often-cited inverse correlation of solvent donicity (enthalpy of solvation) with aggregation number is flawed.[42] In this study, however, the old paradigm holds true.

Despite its complexity, the structure of the aryllithium was successfully controlled as monomer **6** (TMCDA and HMPA) or mixed dimer **7** (THF, *n*-BuOMe, and DME) as required for detailed rate studies.

Monomer-Based Reactivity

In the case of HMPA, solvation by an additional HMPA ligand occurs en route to the transition state. Two solvents eliciting the highest overall reaction rates (eq 1) also foster monomer-based pathways; these results follow conventional wisdom. Previous studies had shown that THF-solvated mixed dimer **7** can rearrange either directly as the mixed dimer or via aryllithium monomer following deaggregation (see **12**). In this instance, the high rates observed at low LDA concentrations arise from the monomer-based rearrangement. Overall, as one might expect, the two solvents that afford observable monomers even in the presence of excess LDA also promote reaction via monomer-based transition structures.

Mixed Dimer-Based Reactivity

Mixed dimers are reactive forms for all of the ethereal solvents (although not exclusively so). The results in THF present an interesting mechanistic issue. A first-order THF dependence affiliated with the mixed dimer-based reaction suggests that a disolvated dimer-based pathway is operative (eq 3). Computations reveal that one of the reasonable transition structures has an affiliated expanded ring resulting from chelation by the meta fluoro group. This expanded ring is illustrated in transition structure **26**. We expressed some concern (vide supra) that the stability of such open dimers may be over-stated, but we find them interesting.

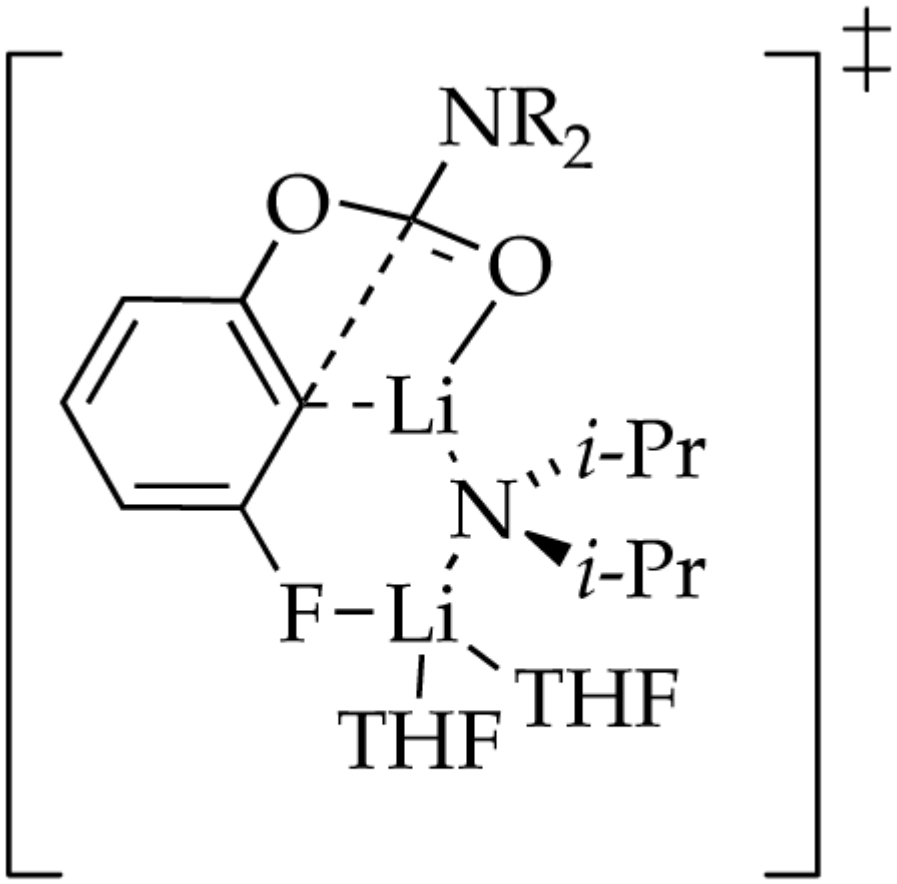

26

A similar effect shows up in rearrangements using DME. Binding studies show that DME and *n*-BuOMe are nearly equivalent ligands toward mixed dimer **7**, whereas *rate* studies show that the rearrangement is 90 times faster in DME (eq 1). We infer, therefore, that DME is *not* chelated in the reactant but *is* chelated in the transition structure (eq 22). Marked rate accelerations stemming from the hemilability of DME are well documented for LDA-mediated metalations.[38] Computations suggest that the rearrangement proceeds via open dimer **27**. We hasten to add, however, that the computations exaggerated the stability of such an open dimer motif in the reactant. Nonetheless, this role of the meta substituent certainly provokes thought.

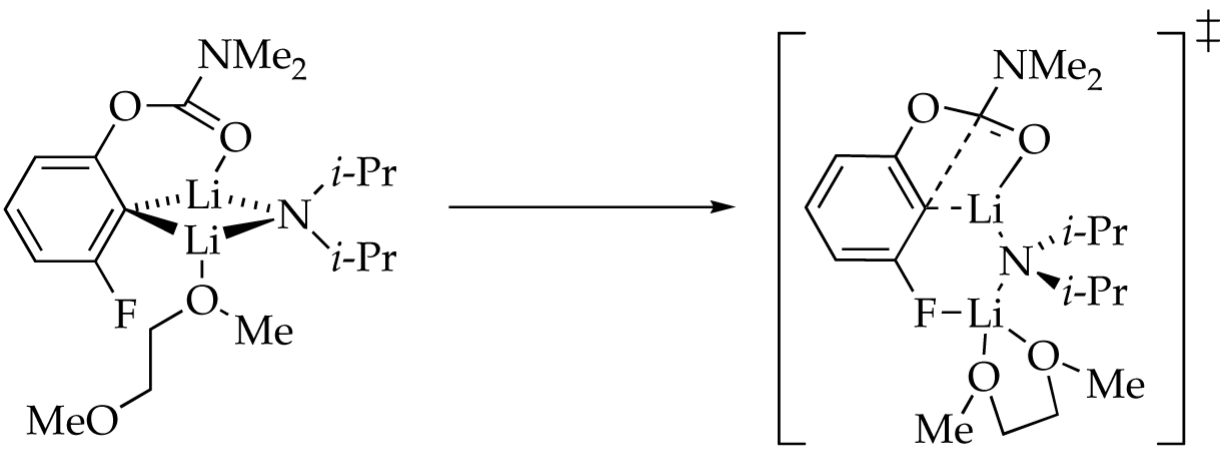

7e **27**

(22)

Mixed Trimer-Based Reactivity

Metalations in *n*-BuOMe in which mixed dimer **7** is the observable reactant displayed an unusual (possibly unprecedented[11]) half order LDA dependence affiliated with a non-zero intercept. The intercept signifies a pathway requiring no LDA dissociation from mixed dimer **7**, which implicates a mixed dimer-based pathway as discussed above. The half-order dependence, in conjunction with a zeroth-order *n*-BuOMe dependence, suggests a rearrangement mechanism requiring *an additional equivalent of LDA monomer*. The stoichiometry must be that of a mixed trimer, $[(i\text{-Pr}_2\text{NLi})_2(\text{ArLi})(n\text{-BuOMe})]^{\ddagger}$.[14] Of the >100 rate laws measured for LDA-mediated reactions to date,[11] we have not observed evidence of trimer- or mixed trimer-based reactivity. Moreover, we are unaware of any documented case of an organolithium reaction proceeding through a higher aggregation state than that observed for the reactants.[13] It is also interesting that simply changing from THF to *n*-BuOMe, arguably a fairly subtle change, causes the rearrangement to change from LDA inhibited to LDA promoted.

Conclusions

Studies of ortholithiated aryl carbamates show that changes in solvent afford marked shifts in structure from aryllithium monomer to LDA-aryllithium mixed dimers and trimers. The mechanisms of the subsequent Snieckus-Fries rearrangements underscore a similar structural diversity in the rate limiting transition structures. In addition to the insights offered into the intimate interplay between solvent and substrate to control solution structure and reaction mechanism, one finds several surprising observations. The meta substituent on the aryl ring may play role in the rearrangement beyond simply stabilizing the aryllithium. Given the importance of substituted aryllithiums in synthesis,[1,45] such an observation may be of significance. Also, an odd variant of hemilability[46]--the penchant for bifunctional ligands to accelerate organolithium reactions by chelating only in the rate-limiting transition state[38,47]--seems to have surfaced. As a final summarizing note, evidence that an observable mixed dimer undergoes further aggregation to mixed trimer, once again, suggests that the correlation of aggregation state and reactivity requires some care. Thus, one is reminded that relationships among product yields, reaction rates, aggregate structures, and reaction mechanisms are often quite complex.

Experimental Section

Reagents and Solvents

THF, *n*-BuOMe, DME, Me_2NEt, hexane, toluene, and pentane were distilled from blue or purple solutions containing sodium benzophenone ketyl. The hydrocarbon stills contained 1% tetraglyme to dissolve the ketyl. HMPA was dried over CaH_2 and vacuum distilled. TMEDA and TMCDA were recrystallized as their HCl salts[39,48] and distilled from blue or purple solutions containing sodium benzophenone ketyl. Owing to evidence that commercially available *R,R*- and *S,S*-cyclohexanediamine may contain impurities that influence reaction rates, we resolved racemic *trans*-1,2-cyclohexanediamine following literature procedures.[39] LDA, [^{6}Li]LDA, and [^{6}Li,^{15}N]LDA were prepared from *n*-BuLi and *i*-Pr_2NH and recrystallized.[15] Air- and moisture-sensitive materials were manipulated under argon or nitrogen using standard glovebox, vacuum line, and syringe techniques. Solutions of *n*-BuLi and LDA were titrated using a literature method.[49] Aryl carbamates **4a**-**e** were prepared by literature procedures.[18]

NMR Spectroscopic Analyses

Standard ^{1}H and ^{13}C spectra were recorded on a 300 MHz spectrometer. ^{1}H, ^{6}Li, ^{13}C, and ^{15}N NMR spectra were recorded on a 400, 500, or 600 MHz spectrometers. The ^{6}Li and ^{15}N resonances are referenced to 0.30 M [^{6}Li]LiCl/MeOH at -90 °C (0.0 ppm) and neat Me_2NEt at -90 °C (25.7 ppm), respectively. The ^{13}C resonances are referenced to the CH_2O resonance of THF at -90 °C (67.6 ppm), the ipso resonance of toluene at 137.9 ppm, and methyl resonance of pentane at 14.1 ppm.

IR Spectroscopic Analyses

Spectra were recorded using an in situ IR spectrometer fitted with a 30-bounce, silicon-tipped probe. The spectra were acquired in 16 scans at a gain of 1 and a resolution of 8 cm^{-1}. A representative reaction was carried out as follows: The IR probe was inserted through a nylon adapter and O-ring seal into an oven-dried, cylindrical flask fitted with a magnetic stir bar and a T-joint. The T-joint was capped by a septum for injections and a nitrogen line. Following evacuation under a full vacuum, heating, and flushing with nitrogen, the flask was charged with LDA (25 mg to 500 mg) in a solvent/co-solvent solution (9.9 mL) and cooled in a temperature-controlled bath. After recording a background spectrum, a carbamate was added to the LDA/solvent/co-solvent mixture from a dilute stock solution (100 μL, 0.400 M) with stirring. IR spectra were recorded over the course of the reaction. To account for mixing and temperature equilibration, spectra recorded in the first 1.5 min were discarded. All reactions were monitored to >5 half-lives.

Supplementary Material

Refer to Web version on PubMed Central for supplementary material.

Acknowledgments

We thank the National Institutes of Health for direct support of this work and Merck, Pfizer, Boehringer-Ingelheim, R. W. Johnson, Aventis, Schering-Plough, and DuPont Pharmaceuticals (Bristol-Myers Squibb) for indirect support. We also thank Emil Lobkovsky for help with a crystal structure determination.

References and Footnotes

1. Hartung, CG.; Snieckus, V. Modern Arene Chemistry. Astruc, D., editor. Wiley-VCH; Weinheim: 2002. Chapter 10 (b) Snieckus V. Chem. Rev 1990;90:879. (c) Taylor CM, Watson AJ. Curr. Org. Chem 2004;8:623.

2. Sibi MP, Snieckus V. J. Org. Chem 1983;48:1935.

3. LDA = lithium diisopropylamide (LDA); DME = 1,2-dimethoxyethane; TMEDA = *N,N,N',N'*-tetramethylethylenediamine; TMCDA = *trans-N,N,N',N'*-tetramethylcyclohexanediamine (optically pure *R,R* or *S,S* enantiomer); and HMPA = hexamethylphosphoramide.

4(a). The Lewis acid-mediated version was discovered by Fries in 1908.[5a] A photochemical variant was first described in 1960,[5b] and the anionic variant appears to have been first reported by Melvin in 1981.[5c] Snieckus reported the first anionic Fries rearrangement of an aryl carbamate in 1983.[2]

5. (a) Fries K, Finck G. Ber 1908;41:2447. (b) Anderson JC, Reese CB. Proc. Chem. Soc 1960:217. (c) Melvin LS. Tetrahedron Lett 1981:3375.

6. Industrial applications:(a) Nguyen T, Wicki MA, Snieckus V. J. Org. Chem 2004;69:7816. [PubMed: 15527256] (b) Mhaske SB, Argade NP. J. Org. Chem 2004;69:4563. [PubMed: 15202923] (c) Harfenist M, Joseph DM, Spence SC, Mcgee DPC, Reeves MD, White HL. J. Med. Chem 1997;40:2466. [PubMed: 9258353] (d) Pietrre A, Chevenier E, Massardier C, Gimbert Y, Greene AE. Org. Lett 2002;4:3139. [PubMed: 12201736] (e) Dankwardt JW. J. Org. Chem 1998;63:3753. (f) Mohri S, Stefinovic M, Snieckus V. J. Org. Chem 1997;62:7072. [PubMed: 11671798] (g) Lampe JW, Hughes PF, Biggers CK, Smith SH, Hu H. J. Org. Chem 1994;59:5147. (h) Ding F, Zhang Y, Qu B, Li G, Farina V, Lu BZ, Senanayake CH. Org. Lett 2008;10:1067. [PubMed: 18275207]

7. (a) Singh KJ, Collum DB. J. Am. Chem. Soc 2006;128:13753. [PubMed: 17044703] (b) Ma Y, Collum DB. J. Am. Chem. Soc 2007;129:14818. [PubMed: 17985891]

8. (a) Kauch M, Hoppe D. Can. J. Chem 2001;79:1736. (b) Kauch M, Snieckus V, Hoppe D. J. Org. Chem 2005;70:7149. [PubMed: 16122233]

9. Collum DB. Acc. Chem. Res 1992;25:448.

10. (a) Bernstein MP, Collum DB. J. Am. Chem. Soc 1993;115:8008. (b) Sun X, Collum DB. J. Am. Chem. Soc 2000;122:2452. (c) Zhao P, Collum DB. J. Am. Chem. Soc 2003;125:14411. [PubMed: 14624589]

11. Collum DB, McNeil AJ, Ramirez A. Angew. Chem., Int. Ed 2007;46:3002.

12. For leading references and discussions of mixed aggregation effects, see:(a) Seebach D. Angew. Chem., Int. Ed. Engl 1988;27:1624.(b)TchoubarBLoupyASalt Effects in Organic and Organometallic Chemistry1992VCHNew YorkChapters 4, 5, and 7 (c) Briggs TF, Winemiller MD, Xiang B, Collum DB. J. Org. Chem 2001;66:6291. [PubMed: 11559177] (d) Caubere P. Chem. Rev 1993;93:2317. (e) Gossage RA, Jastrzebski JTBH, van Koten G. Angew. Chem., Int. Ed 2005;44:1448.(f)SeebachD93Proceedings of the Robert A. Welch Foundation Conferences on Chemistry and BiochemistryWiley: New York1984

13. The exchange of free and bound TMEDA on a TMEDA-chelated lithium amide monomer appears to proceed by dimer-based mechanism:Lucht BL, Bernstein MP, Remenar JF, Collum DB. J. Am. Chem. Soc 1996;118:10707.

14. The rate law provides the stoichiometry of the transition structure relative to that of the reactants:Edwards JO, Greene EF, Ross J. J. Chem. Educ 1968;45:381.

15. Kim Y-J, Bernstein MP, Galiano-Roth AS, Romesberg FE, Fuller DJ, Harrison AT, Collum DB, Williard PG. J. Org. Chem 1991;56:4435.

16. The spins of ^{6}Li, ^{13}C, and ^{15}N are 1, 1/2, and 1/2, respectively.

17. (a) Collum DB. Acc. Chem. Res 1993;26:227. (b) Remenar JF, Lucht BL, Collum DB. J. Am. Chem. Soc 1997;119:5567. (c) Bernstein MP, Romesberg FE, Fuller DJ, Harrison AT, Williard PG, Liu QY, Collum DB. J. Am. Chem. Soc 1992;114:5100. (d) Romesberg FE, Gilchrist JH, Harrison AT, Fuller DJ, Collum DB. J. Am. Chem. Soc 1991;113:5751.

18. (a) Lustig E, Benson WR, Duy N. J. Org. Chem 1967;32:851. (b) Yamagami C, Takao N, Nishioka T, Fujita T, Takeuchi Y. Org. Magn. Reson 1984;22:439.

19. Rutherford JL, Collum DB. J. Am. Chem. Soc 1999;121:10198.

20. Xiang B, Winemiller MD, Briggs TF, Fuller DJ, Collum DB. Magn. Reson. Chem 2001;39:137.

21. Singh, KJ.; Hoepker, AC.; Collum, DB. Cornell University; Ithaca, N.Y.: Unpublished work

22. For a discussion and leading references to the use of mixed aggregation to provide insight into homoaggregation, see ref [47b].

23. (a) Ramirez A, Candler J, Bashore CG, Wirtz MC, Coe JW, Collum DB. J. Am. Chem. Soc 2004;126:14700. [PubMed: 15535677] (b) Riggs JC, Ramirez A, Cremeens ME, Bashore CG,

Candler J, Wirtz MC, Coe JW, Collum DB. J. Am. Chem. Soc 2008;130:3406. [PubMed: 18293971] (c) Stratakis M, Wang PG, Streitwieser A. J. Org. Chem 1996;61:3145. [PubMed: 11667177] (d) Reich HJ, Green DP, Medina MA, Goldenberg WS, Gudmundsson BÖ, Dykstra RR, Phillips NH. J. Am. Chem. Soc 1998;120:7201.

24. (a) Crittendon RC, Beck BC, Su J, Li XW, Robinson GH. Organometallics 1999;18:156. (b) Olmstead MM, Power PP. J. Organomet. Chem 1999;408:1. (c) Girolami GS, Riehl ME, Suslick KS, Wilson SR. Organometallics 1992;11:3907. (d) Bosold F, Zulauf P, Marsch M, Harms K, Lohrenz J, Boche G. Angew. Chem., Int. Ed 1991;30:1455. (e) Hardman NJ, Twamley B, Stender M, Baldwin R, Hino S, Schiemenz B, Kauzlarich SM, Power PP. J. Organomet. Chem 2002;643:461. (f) Wegner GL, Berger RJF, Schier A, Schmidbaur H. Z. Naturforsch., B: Chem. Sci 2000;55:995. (g) Schiemenz B, Power PP. Angew. Chem., Int. Ed 1996;35:2150. (h) Maetzke T, Seebach D. Helv. Chim. Acta 1989;72:624. (i) Kottke T, Sung K, Lagow RJ. Angew. Chem., Int. Ed 1995;34:1517.
25. For representative computational studies of aryllithiums, see:(a) Krasovsky A, Straub BF, Knochel P. Angew. Chem., Int. Ed. Engl 2006;45:159. (b) Bachrach SM, Chamberlin AC. J. Org. Chem 2004;69:2111. [PubMed: 15058960] (c) Kwon O, Sevin F, McKee ML. J. Phys. Chem. A 2001;105:913. (d) Wiberg KB, Sklenak S, Bailey WF. J. Org. Chem 2000;65:2014. [PubMed: 10774021] (e) Kremer T, Junge M, Schleyer P. v. R. Organometallics 1996;15:3345.(f) Also, see ref 23b.
26. (a) Menzel K, Fisher EL, DiMichele L, Frantz DE, Nelson TD, Kress MH. J. Org. Chem 2006;71:2188. [PubMed: 16497017](b) $^{2}J_{C\text{-}F}$ values have been correlated with ·-bond orders and total electronic charge at the ^{13}C atom:Doddrell D, Barfield M, Adcock W, Aurangzeb M, Jordan D. J. Chem. Soc., Perkin Trans. 2 1976:402.
27. The homoaggregated phenolates tend to be insoluble, and their often-complex structures in solution are unknown. Structurally analogous lithium phenolates bearing carbonyl-containing moieties in the ortho position have been characterized crystallographically:(a) Wang Z, Chai Z, Li Y. J. Organomet. Chem 2005;690:4252. (b) Boyle TJ, Pedrotty DM, Alam TM, Vick SC, Rodriguez MA. Inorg. Chem 2000;39:5133. [PubMed: 11233212] (c) Clegg W, Lamb E, Liddle ST, Snaith R, Wheatley AEH. J. Organomet. Chem 1999;573:305. (d) Cetinkaya B, Gumrukcu I, Lappert MF, Atwood JL, Shakir R. J. Am. Chem. Soc 1980;102:2086. (e) Khanjin NA, Menger FM. J. Org. Chem 1997;62:8923.
28. Hsieh, HL.; Quirk, RP. Anionic Polymerization: Principles and Practical Applications. Marcel Dekker; New York: 1996. Wardell, JL. Comprehensive Organometallic Chemistry. Wilkinson, G.; Stone, FGA.; Abel, EW., editors. 1. Pergamon; New York: 1982. Chapter 2Szwarc, M., editor. Ions and Ion Pairs in Organic Reactions. I-II. Wiley; New York: 1972.
29. Espenson, JH. Chemical Kinetics and Reaction Mechanisms. 2nd ed.. McGraw-Hill; New York: 1995.
30. Rein AJ, Donahue SM, Pavlosky MA. Curr. Opin. Drug Discov. Dev 2000;3:734.
31. The concentration of the LDA, although expressed in units of molarity, refers to the concentration of the monomer unit (normality). The concentrations of solvent are expressed as total concentration of free (uncoordinated) form.
32. Briggs TF, Winemiller MD, Collum DB, Parsons RL Jr. Davulcu AK, Harris GD, Fortunak JD, Confalone PN. J. Am. Chem. Soc 2004;126:5427. [PubMed: 15113214]
33. Frisch, MJ., et al. *Gaussian 03*; revision B.04. Gaussian, Inc.; Wallingford, CT: 2004. Dennington, R., II; Keith, T.; Millam, J.; Eppinnett, K.; Hovell, WL.; Gilliland, R. GaussView, Version 3.09. Semichem, Inc.; Shawnee Mission, KS: 2003.
34. We define the idealized rate law as that obtained by rounding the observed reaction orders to the nearest rational order.
35. Romesberg FE, Collum DB. J. Am. Chem. Soc 1994;116:9198.
36. (a) Reich HJ, Kulicke KJ. J. Am. Chem. Soc 1995;117:6621. (b) Reich HJ, Green DP, Medina MA, Goldenberg WJ, Gudmundsson BÖ, Dykstra RR, Philips NH. J. Am. Chem. Soc 1998;120:7201. (c) Reich HJ, Sikorski WH, Gudmundsson BÖ, Dykstra RR. J. Am. Chem. Soc 1998;120:4035. (d) Reich HJ, Holladay JA, Mason JD, Sikorski WH. J. Am. Chem. Soc 1995;117:12137. (e) Reich HJ, Borst JP, Dykstra RR, Green DP. J. Am. Chem. Soc 1993;115:8728. (f) Jantzi KL, Puckett CL, Guzei IA, Reich HJ. J. Org. Chem 2005;70:7520. [PubMed: 16149779]and references cited therein.
37. See ref 10c and references cited therein.

38. (a) Ramirez A, Collum DB. J. Am. Chem. Soc 1999;121:11114. (b) Ramirez A, Lobkovsky E, Collum DB. J. Am. Chem. Soc 2003;125:15376. [PubMed: 14664582] (c) Remenar JF, Collum DB. J. Am. Chem. Soc 1997;119:5573.

39(a). We found that TMCDA prepared from commercially available *R,R*- and *S,S*-1,2-cyclohexanediamines did not afford equivalent rates of rearrangement. Although the source of the differences was not found, we alleviated the problem by resolving *trans*-cyclohexanediamine,[39b] N-methylating the methyls,[17b] and re-crystallizing the resulting TMCDA as its HCl salt.[17b] We found that the optical purity of *trans*-1,2-cyclohexanediamine and TMCDA could be evaluated by ^{13}C NMR spectroscopy by adding two equiv of (+)-taddol in toluene-d_8.[39c](b) Larrow JF, Jacobsen EN. Org. Synth 1998;10:96. (c) Seebach D, Beck AK, Heckel A. Angew. Chem., Int. Ed 2001;40:92.

40. (a) Lucht BL, Collum DB. J. Am. Chem. Soc 1996;118:2217. (b) Settle FA, Haggerty M, Eastham JF. J. Am. Chem. Soc 1964;86:2076. (c) Lewis HL, Brown TL. J.Am.Chem.Soc 1970;92:4664. (d) Brown TL, Gerteis RL, Rafus DA, Ladd JA. J. Am. Chem. Soc 1964;86:2135. (e) Quirk RP, Kester DE. J. Organomet. Chem 1977;127:111.

41. Lucht BL, Collum DB. Acc. Chem. Res 1999;32:1035.

42. Sun X, Collum DB. J. Am. Chem. Soc 2000;122:2459.Also, see ref [9].

43. Lucht BL, Bernstein MP, Remenar JF, Collum DB. J. Am. Chem. Soc 1996;118:10707.

44. (a) Bauer W, Klusener PAA, Harder S, Kanters JA, Duisenberg AJM, Brandsma L, Schleyer P. v. R. Organometallics 1988;7:552. (b) Köster H, Thoennes D, Weiss E. J. Organomet. Chem 1978;160:1. (c) Tecle' B, Ilsley WH, Oliver JP. Organometallics 1982;1:875. (d) Harder S, Boersma J, Brandsma L, Kanters JA. J. Organomet. Chem 1988;339:7. (e) Sekiguchi A, Tanaka M. J. Am. Chem. Soc 2003;125:12684. [PubMed: 14558797] (f) Linnert M, Bruhn C, Ruffer T, Schmidt H, Steinborn D. Organometallics 2004;23:3668. (g) Fraenkel G, Stier M. Prepr. Am. Chem. Soc., Div. Pet. Chem 1985;30:586. (h) Ball SC, Cragg-Hine I, Davidson MG, Davies RP, Lopez-Solera MI, Raithby PR, Reed D, Snaith R, Vogl EM. J. Chem. Soc., Chem. Commun 1995:2147. (i) Wehman E, Jastrzebski JTBH, Ernsting J-M, Grove JM, van Koten GJ. Organomet. Chem 1988;353:145. (j) Becker J, Grimme S, Fröhlich R, Hoppe D. Angew. Chem., Int. Ed 2007;46:1645.(k) Also, see ref [17c].

45. Gribble, GW. Science of Synthesis. 8.1.14. Georg Thieme Verlag; New York: 2005. Clayden, J. Organolithiums: Selectivity for Synthesis. Pergamon; New York: 2002. Schlosser, M. Organometallics in Synthesis: A Manual. 2nd ed.. Schlosser, M., editor. John Wiley; Chichester: 2002. Chapter 1Clayden, J. The Chemistry of Organolithium Compounds. Rappoport, Z.; Marek, I., editors. 1. Wiley; New York: 2004. p. 495

46. For reviews of hemilabile ligands, see:(a) Braunstein P, Naud F. Angew. Chem., Int. Ed. Engl 2001;40:680. [PubMed: 11241595] (b) Slone CS, Weinberger DA, Mirkin CA. Progr. Inorg. Chem 1999;48:233. (c) Lindner E, Pautz S, Haustein M. Coord. Chem. Rev 1996;155:145. (d) Bader A, Lindner E. Coord. Chem. Rev 1991;108:27.

47. (a) Ramirez A, Sun X, Collum DB. J. Am. Chem. Soc 2006;128:10326. [PubMed: 16881665] (b) Liou LR, McNeil AJ, Ramirez A, Toombes GES, Gruver JM, Collum DB. J. Am. Chem. Soc 2008;130:4859. [PubMed: 18336025]

48. (a) Rennels RA, Maliakal A, Collum DB. J. Am. Chem. Soc 1998;120:421. (b) Freund M, Michaels H. Ber 1897;30:1374.

49. Kofron WG, Baclawski LM. J. Org. Chem 1976;41:1879.

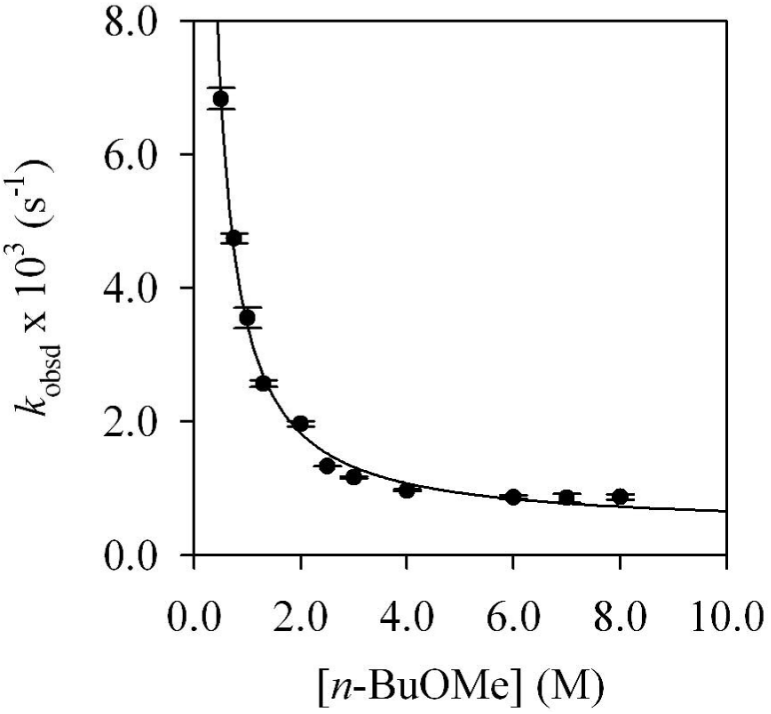

Figure 1.
Plot of k_{obsd} versus [*n*-BuOMe] in pentane cosolvent for the rearrangement of **7d** (0.004 M) by LDA (0.075 M) at 15 °C. The curve depicts an unweighted least-squares fit to $k_{obsd} = k[n\text{-BuOMe}]^n + k'$ ($k = (3.0 \pm 0.1) \times 10^{-3}$, $n = -1.10 \pm 0.05$, $k' = (4.1 \pm 0.1) \times 10^{-4}$).

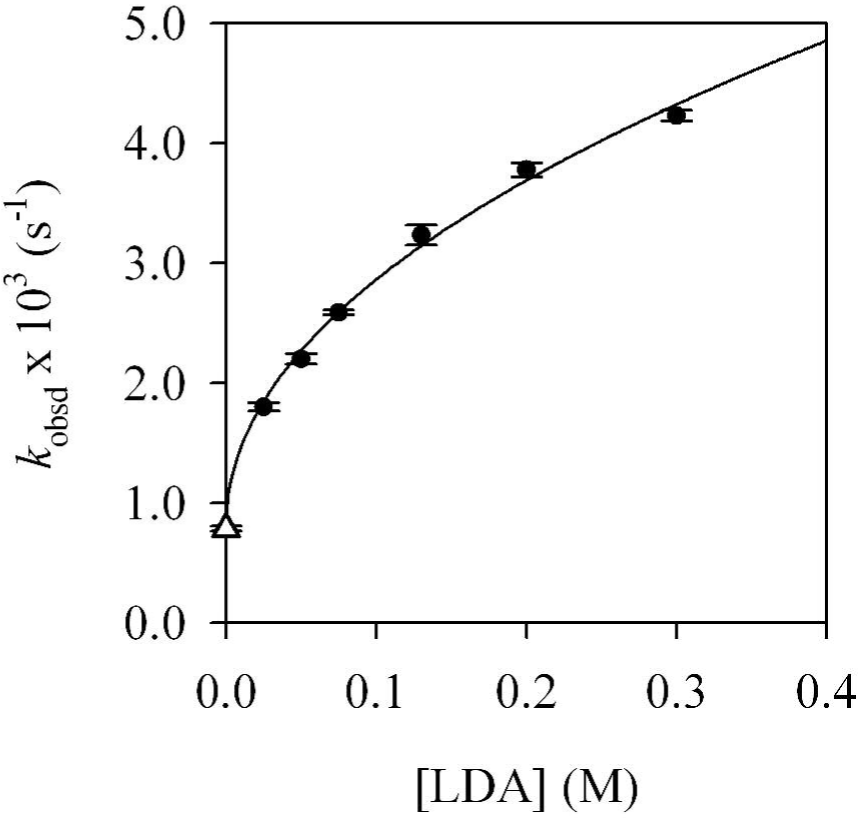

Figure 2.
Plot of k_{obsd} versus [LDA] in 1.3 M *n*-BuOMe/pentane for the rearrangement of **7d** (0.004 M) at 15 °C. The curve depicts an unweighted least-squares fit to $k_{obsd} = k[LDA]^n + k'$ (k = (6.3 ± 0.2) × 10^{-3}, n = 0.49 ± 0.09, k' = (7.9 ± 0.2) × 10^{-4}). k' (see ·) was set to equal k' in Figure 3.

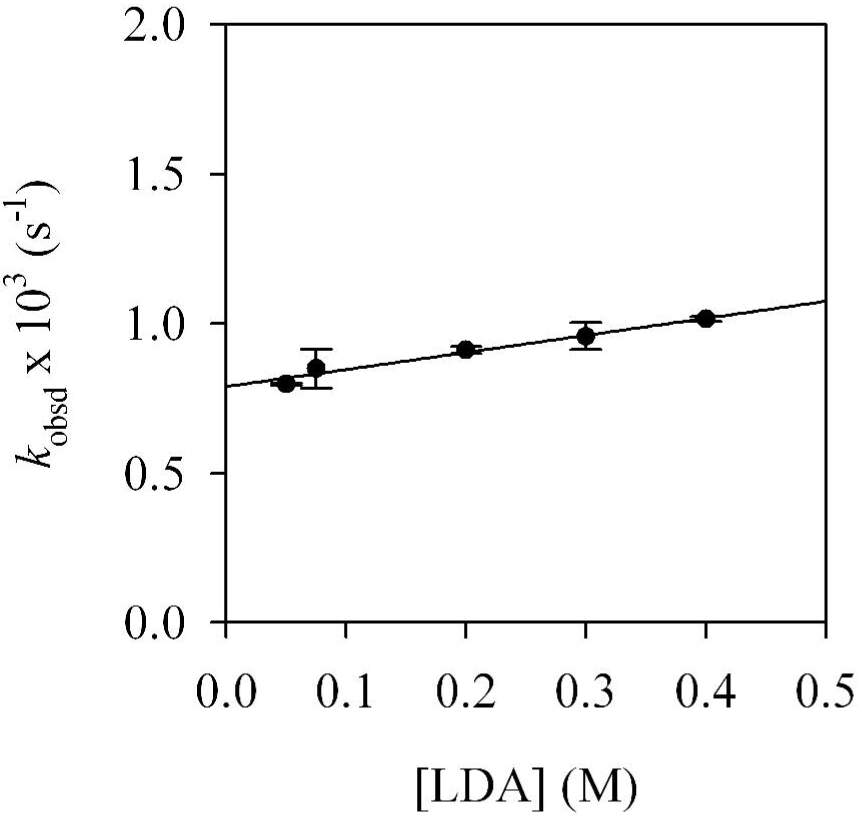

Figure 3.
Plot of k_{obsd} versus [LDA] in 7.0 M *n*-BuOMe/pentane for the rearrangement of **7d** (0.004 M) at 15 °C. The curve depicts an unweighted least-squares fit to $k_{obsd} = k[LDA] + k'$ ($k = (5.7 \pm 0.8) \times 10^{-4}$, $k' = (7.9 \pm 0.2) \times 10^{-4}$).

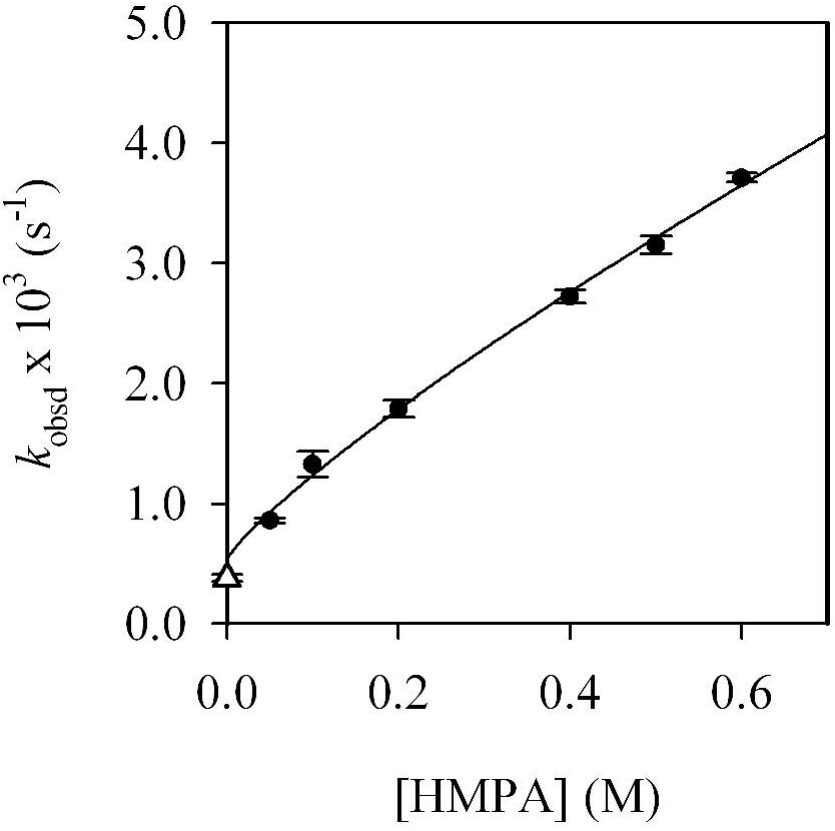

Figure 4.

Plot of k_{obsd} versus [HMPA] in 10.0 M THF/hexanes cosolvent for the rearrangement of **6b** (0.004 M) by LDA (0.10 M) at -65 °C. The curve depicts an unweighted least-squares fit to $k_{obsd} = k[\text{HMPA}]^n + k'$ ($k = (4.8 \pm 0.2) \times 10^{-3}$, $n = 0.8 \pm 0.1$, $k' = (0.5 \pm 0.2) \times 10^{-3}$). Pseudo-first-order conditions not maintained at 0.05 M HMPA (·); data was omitted from the fit.

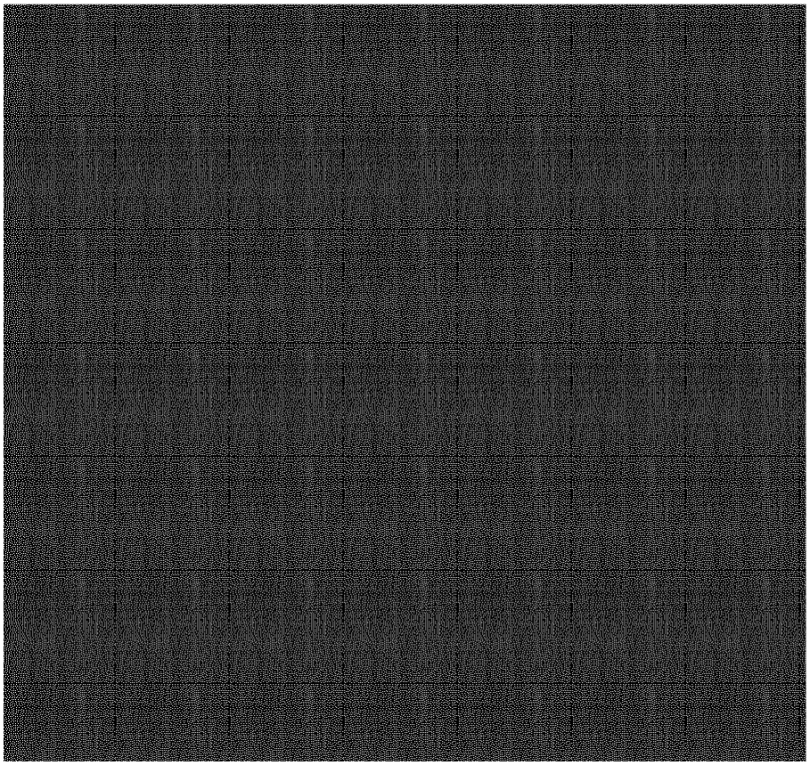

Figure 5.
Theoretical curves describing k_{obsd} versus mole fraction of DME (X_{DME}) according to eq 16 for mixtures of *n*-BuOMe and DME. The assumed values of K_{eq} are as labeled. The relative rate constants for k_{BuOMe} and k_{DME} correspond to the left and right *y*-intercepts and arbitrarily assigned as 0.05 and 1.1, respectively.

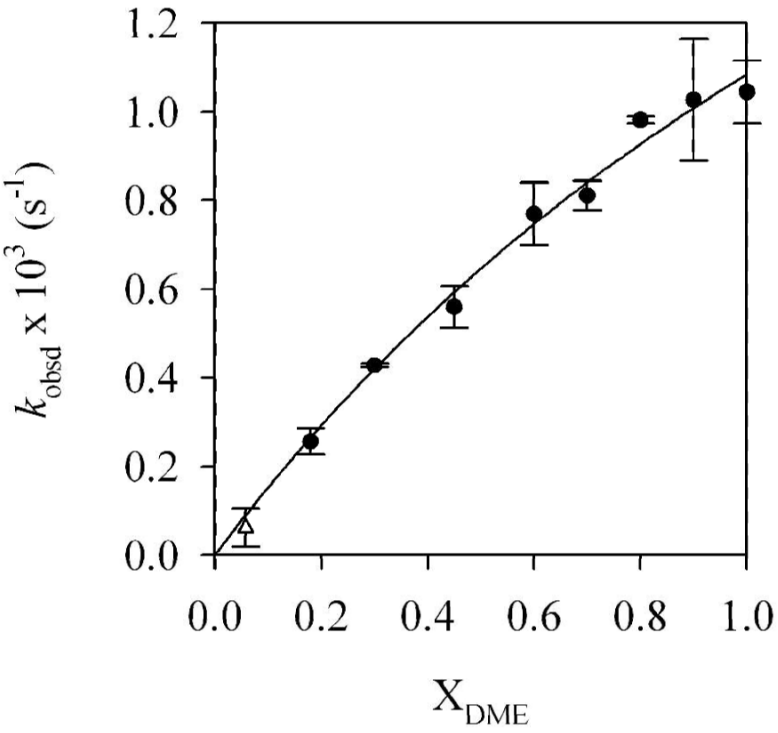

Figure 6.

Plot of k_{obsd} versus mole fraction of DME (X_{DME}) for the rearrangement of **7e** (0.004 M) by LDA (0.05 M) at -60 °C. The donor solvent concentration is held constant ([DME]+[*n*-BuOMe] =5.0 M) using pentane as cosolvent. The curve depicts an unweighted least-squares fit to $k_{obsd} = (a + bx)/(1 + cx)$ ($a = (0.0 \pm 0.1) \times 10^{-3}$, $b = 1.6 \pm 0.5$, $c = 0.5 \pm 0.4$) such that $1 + c = K_{eq}$ (see eq 16). At low DME concentrations the lithium phenolate precipitated during the reaction; the value of k_{obsd} (shown as *) was not included in the fit.

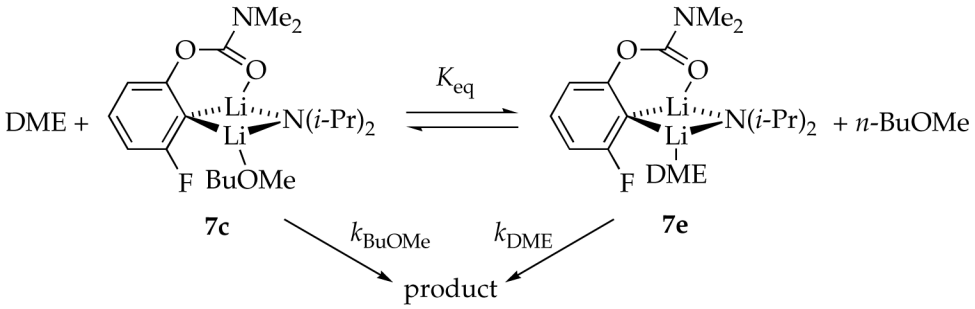

Scheme 1.

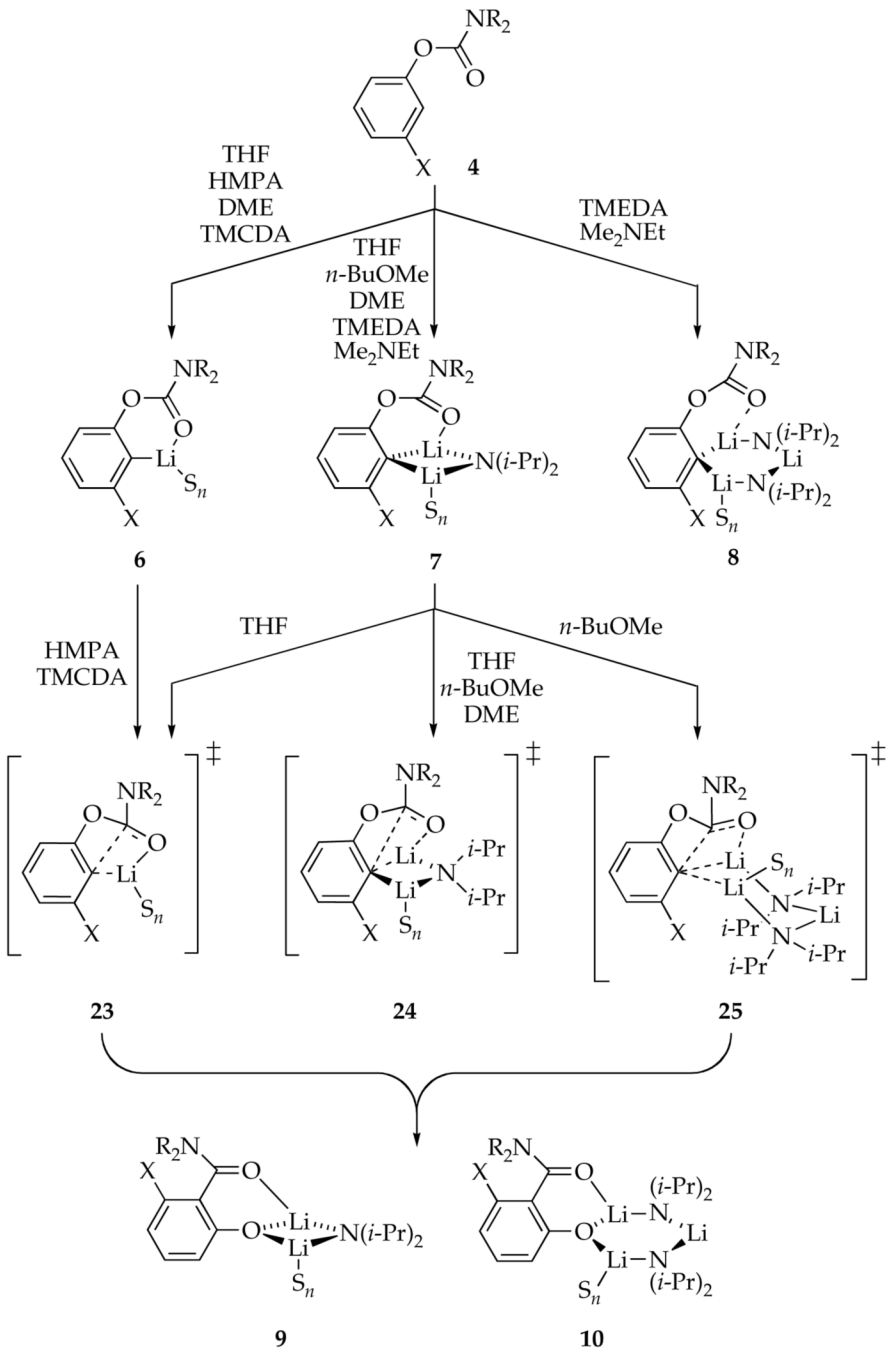

Scheme 2.

Table 1

^{6}Li and ^{15}N NMR spectroscopic data[a,b]

ArLi	Solvent	R	X	^{6}Li, δ (mult,$^{1}J_{LiN}$	^{15}N, δ(mult)
6a[c]	THF	*i*-Pr	F	1.23 (s)	--
6c[b]	HMPA	*i*-Pr	OMe	0.91 (s)	--
6e	HMPA	*i*-Pr	F	0.75 (s)	--
6f[c,b]	DME	*i*-Pr	F	1.65 (s)	--
6g[b]	TMCDA	Et	OMe	2.18 (s)	--
7b[b]	THF	*i*-Pr	F	1.71 (d, 5.3)	76.3 (q)
7d[b]	*n*-BuOMe	Et	OMe	1.85 (d, 5.8)	75.8 (q)
7f[b]	DME	*i*-Pr	F	1.60 (d, 5.4)	75.2 (q)
7g	TMEDA	*i*-Pr	OMe	2.01 (d, 4.9)	75.3 (q)
7h	Me_2NEt	Et	OMe	1.93 (d,5.2)	75.3 (q)
8a	TMEDA	*i*-Pr	OMe	0.78 (d, 5.7) 2.49 (t, 4.7) 2.50 (d, 5.7)	73.8 (tt) 75.3 (q)
8b	Me_2NEt	Et	OMe	0.81 (d, 6.3) 2.24 (d, 6.0) 2.80 (t, 4.9)	74.2 (tt) 74.3 (q)
9a	THF	Me	F	0.40 (d, 4.8)	79.1 (q)
9b	*n*-BuOMe	Et	OMe	0.93 (d, 4.9)	75.1 (q)
9c	HMPA	Et	OMe	0.54 (d, 5.3)	76.5 (q)
9d	HMPA	Me	F	0.66 (d, 4.6)	76.3 (q)
10a	*n*-BuOMe	Et	OMe	1.49 (d, 5.5) 1.55 (d, 6.2) 1.89 (t, 5.2)	74.4 (--)[d] 74.1 (--)[d]
10b	HMPA	Et	OMe	1.09 (d, 5.3) 1.12 (d, 5.3) 1.58 (t, 4.6)	73.2 (--)[d] 74.7 (tt)
10c	DME	Me	F	0.95 (d, 4.7) 0.98 (d, 5.1) 1.82 (t, 5.1)	72.9 (q) 74.3 (q)
10d	TMEDA	Me	OMe	1.21 (d, 5.0) 1.67 (t, 4.9)	74.9 (q) 75.1 (q)
10e	Me_2NEt	Et	OMe	1.79 (d, 6.2) 1.79 (t, 5.1) 1.84 (d, 6.1)	73.8 (tt) 74.3 (tt)

[a] Multiplicities are denoted as follows: s, singlet; d, doublet; t, triplet; q, quintet. The chemical shifts are reported relative to 0.30 M ^{6}LiCl/MeOH (δ 0.0 ppm) and neat Me_2NEt (δ 25.7 ppm) at -90 °C. ^{13}C NMR spectra are referenced to toluene-*d*8 (δ 137.9 ppm), pentane (δ 14.1 ppm), or THF (δ 67.6 ppm). Chemical shifts are reported in ppm, and *J* values are reported in Hz.

[b] Carbon-13 resonances of the carbanionic carbons: **6c**, δ 158.7 (br s); **6f**, δ 150.1 (br d, J_{FC}=7.7); **6g**, δ 155.1 (t, J_{CLi}=120.7); **7b**, δ 150.5 (br d, J_{FC}=123); **7d**, δ 155.2 (q, J_{CLi}=5.7); **7f**, δ 154.6 (dq, J_{FC}=123, J_{CLi}=5.9).

[c] 1.0 equiv [^{6}Li,^{15}N]LDA.

[d] Obscured by another resonance.

Table 2

Summary of Rate Studies for the Anionic Snieckus-Fries Rearrangement

ArLi	Solvent	R	X	Temperature °C	LDA Order	Solvent Order
7a	THF	Me	F	-40	0 -0.48±0.04	+1.08±0.05[a] +2.4±0.6[b]
7d	*n*-BuOMe	Et	OMe	15	0[c] +0.49±0.09[d]	0 -1.10±0.05
6b[e]	HMPA	Et	OMe	-65	0	+0.8±0.1
6d[e]	HMPA	Me	F	-78	0	+1.2±0.3
7e	DME	Me	F	-60	0	0
6g	TMCDA	Et	OMe	-25	0	0

[a] 0.42 M LDA.

[b] 0.098 M LDA.

[c] 7.0 M *n*-BuOMe.

[d] 1.3 M *n*-BuOMe.

[e] The order in THF cosolvent is zero.